Title Page

Report Title
Development and deployment of a compact eye-safe scanning differential absorption lidar (DIAL) for spatial mapping of carbon dioxide for monitoring/verification/accounting at geologic sequestration sites

Type of Report
Final Technical Report

Reporting Period
December 1, 2009 – March 31, 2014

Principal Author
Dr. Kevin Repasky

Date of Report
May, 2014

DoE Award Number
DE-FE0001156

Submitting Organization
Montana State University
Electrical and Computer Engineering
Cobleigh Hall Room 610
Bozeman, MT 59717

Disclaimer

Abstract

A scanning differential absorption lidar (DIAL) instrument for monitoring carbon dioxide has been developed. The laser transmitter uses two tunable discrete mode laser diodes (DMLD) operating in the continuous wave (cw) mode with one locked to the online absorption wavelength and the other operating at the offline wavelength. Two in-line fiber optic switches are used to switch between online and offline operation. After the fiber optic switch, an acousto-optic modulator (AOM) is used to generate a pulse train used to injection seed an erbium doped fiber amplifier (EDFA) to produce eye-safe laser pulses with maximum pulse energies of 66 μJ, a pulse repetition frequency of 15 kHz, and an operating wavelength of 1.571 μm. The DIAL receiver uses a 28 cm diameter Schmidt-Cassegrain telescope to collect that backscattered light, which is then monitored using a photo-multiplier tube (PMT) module operating in the photon counting mode.

The DIAL instrument has been operated from a laboratory environment on the campus of Montana State University, at the Zero Emission Research Technology (ZERT) field site located in the agricultural research area on the western end of the Montana State University campus, and at the Big Sky Carbon Sequestration Partnership site located in north-central Montana. DIAL data has been collected and profiles have been validated using a co-located Licor LI-820 Gas Analyzer point sensor.

Table of Contents

Executive Summary

The goal of the research project was to develop and demonstrate a differential absorption lidar (DIAL) capable of measuring range resolved profiles of atmospheric carbon dioxide (CO_2) for surface monitoring at carbon sequestration sites. The DIAL laser transmitter utilizes two discrete mode laser diodes (DMLD) operating in the continuous wave (cw) mode with one locked to the online absorption wavelength via a feed-back control loop that utilizes a optical wavemeter and the other operating at the offline wavelength. The output from each DMLD passes through a switch allowing either the on-line or off-line DMLD to injection seed a commercial erbium doped fiber amplifier (EDFA). Pulsing is achieved by utilizing an acousto-optic modulator (AOM) before the EDFA. The DIAL receiver utilizes a 28 cm diameter Schmidt-Cassegrain telescope to collect the backscattered light that is delivered to a photomultiplier tube (PMT). A discriminator after the PMT allows the detection of single photons and produces a TTL logic pulse that is monitored with a multichannel scaler card. A Labview program has been developed to operate the DIAL instrument and data processing is completed with script written in the Matlab programming environment.

Initial testing of the DIAL instrument was completed from a laboratory environment on the campus of Montana State University. The DIAL instrument was capable of monitoring horizontal CO_2 profiles between 1 and 2.5 km. With initial laboratory testing completed, the DIAL instrument was rebuilt in preparation for field deployment. The DIAL instrument was deployed at the Zero Emission Research Technology (ZERT) field site located on the agricultural research land located on the western end of the Montana State University campus. Data was collected during the summer of 2011 and 2012. Validation of the data was achieved by placing a Licor LI-820 monitor, which measures ambient CO_2 levels at a single point, at different sampling positions below the DIAL's line of sight. Good agreement between the DIAL CO_2 concentration measurement and the Licor point sensor indicated that the DIAL instrument is operating correctly.

With this initial field testing completed, the DIAL instrument was prepared for a month long deployment at the Big Sky Carbon Sequestration Partnership (BSCSP) site. The remote BSCSP site is located in north-central Montana near the town of Sunburst. Because of permitting requirements, no infrastructure was in place during the summer of 2013 when the DIAL instrument was deployed for a thirty day period. The DIAL instrument operated from a cargo trailer and power was supplied using a 1.8 kW generator. Data was collected with the DIAL and validated using the Licor LI-820. Good agreement between the DIAL CO_2 concentration measurements and Licor measurements indicated that the DIAL was operating correctly and is capable of monitoring remote carbon sequestration field sites.

Technical Report

I. Introduction

The goal of the research project was to develop and demonstrate a differential absorption lidar (DIAL) for measuring range resolved carbon dioxide (CO_2) profiles carbon sequestration site monitoring. The goals for the research project are encapsulated in a statement of the project objects from the original proposal. The project objectives included the development, testing, and deployment of a scanning eye-safe diode laser based differential absorption lidar (DIAL) for near surface mapping of carbon dioxide (CO_2) number densities. The development of the CO_2 DIAL built on Montana State University's expertise in developing compact low power, high repetition rate diode laser based DIAL instruments for atmospheric studies. Horizontal testing of the instrument was conducted to determine the performance of the CO_2 DIAL instrument at the Zero Emission Research Technology (ZERT) field site during a controlled release experiment. Montana State University then worked with the Big Sky Carbon Sequestration Partnership to deploy the CO_2 DIAL instrument at a regional carbon sequestration demonstration project. Each of these project objectives have been met, as discussed in this report.

The remainder of this report is organized as follows. Section II contains the theoretical underpinning for the design of the DIAL. The laser transmitter and DIAL receiver and data acquisition program are discussed in section III. Data from the laboratory and field deployments are presented in section IV. Finally, some brief concluding remarks are presented in section V.

II. DIAL Theory

DIAL Equation

Lidar applications utilize properties of scattered light to determine various properties associated with the atmosphere. The number of scattered photons, N(λ,r), collected by the lidar instrument at wavelength λ from range r can be calculated using the lidar equation

$$N(\lambda,r) = N_0(\lambda)\frac{A}{r^2}\Delta r\beta(\lambda,r)T_A^2(\lambda,r)\varepsilon_0(r)\varepsilon_R(\lambda)\varepsilon_D(\lambda) \quad (1)$$

where $N_o(\lambda)$ is the number of photons in the outgoing laser pulse, A is the area of the receiver, $\Delta r = \frac{\tau c}{2}$ is the range bin size, τ is the pulse duration, c is the speed of light, $\beta(\lambda,r)$ is the backscatter coefficient, $T_A^2(\lambda,r)$ is the round trip atmospheric transmission, $\varepsilon_0(r)$ is the geometric overlap function, $\varepsilon_R(\lambda)$ is the receiver optics transmission, and $\varepsilon_D(\lambda)$ is the detector efficiency. The round trip atmospheric transmission can be written

$$T_A^2(\lambda,r) = e^{-2\int_0^r \kappa(\lambda,r')dr'}e^{-2\int_0^r \sigma(\lambda,r')N_d(r')dr'} \quad (2)$$

where $\kappa(\lambda, r)$ is the atmospheric extinction coefficient, $\sigma(\lambda,r)$ is the molecular absorption cross-section, and $N_d(r)$ is the number density of molecules. Assuming the number density for the molecule of interest is constant over a range bin and the online wavelength, λ_{on}, and offline wavelength, λ_{off}, are closely spaced so that the atmospheric extinction, backscatter, and receiver efficiency are equal for the two wavelengths, the number density, $N_d(r)$, can be found by considering the online and offline returns in two adjacent range bins using the DIAL equation

$$N_d(r) = \frac{1}{2\Delta r(\sigma(\lambda_{on},r)-\sigma(\lambda_{off},r))}ln\left(\frac{N(\lambda_{on},r)N(\lambda_{off},r+\Delta r)}{N(\lambda_{on},r+\Delta r)N(\lambda_{off},r)}\right) \quad (3)$$

Absorption Band Selection

In order to quantify the number of absorbing molecules interacting with the lidar pulse that causes the increased attenuation, the value of the absorption cross section at the online and offline wavelengths must be known. It is at this point that a decision must be made about which online and offline wavelengths to use. Several criteria must be met by the wavelengths for the DIAL instrument to be able to make a gas concentration measurement with reasonable accuracy and precision. The online and offline wavelengths' absorption properties must not vary significantly with reasonable changes in atmospheric conditions and the online absorption must be sufficiently strong enough to identify a difference in signal attenuation while not being so strong that all of the lidar pulse light is absorbed before reaching the desired measurement range. It is also desirable that there be a minimum of interference from absorption due to other molecules such as water vapor. In addition, there is also the practical need of all of the photonics components being commercially available to make the measurement. For the DIAL discussed in this report which has been developed for monitoring carbon dioxide, the absorption band near 1.57 μm was chosen for its combination of reasonable absorption strength, and maturity and commercial availability of photonics components developed by the telecommunications industry. Using the Hitran 2008 database, a plot of the atmospheric transmission as a function of wavelength is shown in Figure 1.

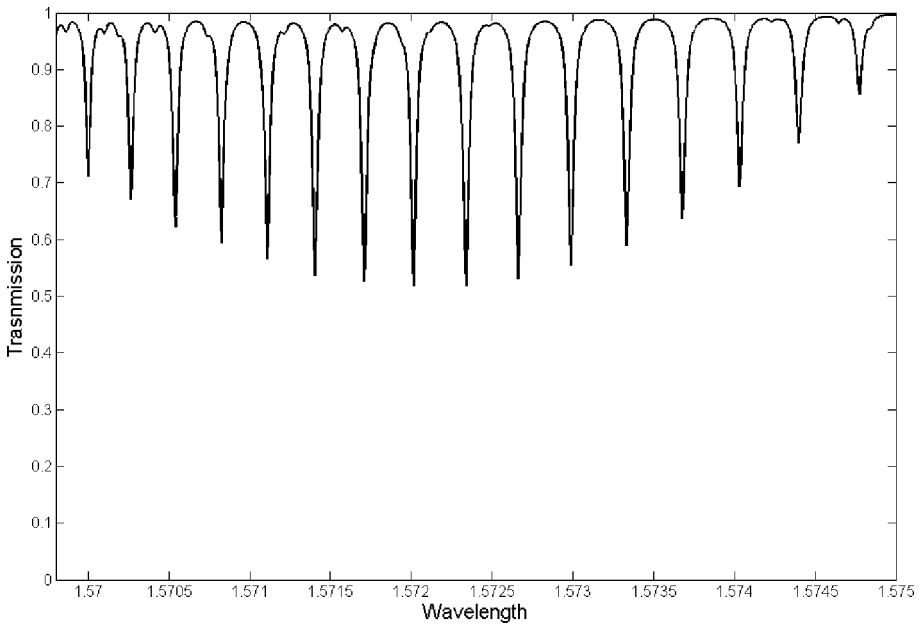

Figure 1 Plot of the atmospheric transmission as a function of wavelength for a path length of 10 km at 296 K, atmospheric pressure of 1 atm, and a CO_2 concentration of 390 ppm.

Absorption Line Selection Criteria

After the decision was made to focus on the 1.57 micron absorption band for the DIAL measurements, a more specific decision about which exact absorption line would be used was made based on the interest of minimizing the absorption sensitivity of the online and offline wavelengths to varying ambient conditions, while maximizing the round trip absorption. To determine which absorption feature within the 1.57 micron band to choose, an examination of

how the round trip absorption is affected by changes in ambient conditions is next discussed. Changes in pressure, temperature, and relative humidity are the strongest sources of round trip absorption variation for a given ambient CO_2 number density. Variations in pressure and temperature directly affect the magnitude of the absorption cross section used to calculate the CO_2 number density, and for that reason accurate knowledge of the magnitude of the absorption cross section at a given pressure and temperature is necessary for accurate DIAL measurements to be made.

The absorption cross section can be calculated with knowledge of the linestrength at the operating temperature T. For the DIAL measurements, a Voight Function, which is a convolution of the Gaussian and Lorentzian lineshapes that result from temperature and pressure broadening respectively, is used. With this absorption lineshape functional form, the absorption cross section is

$$\sigma = S(T)\frac{\ln(2)}{\pi^{3/2}}\frac{\gamma_L}{\gamma_D^2}\int_{-\infty}^{\infty}\frac{e^{-t^2}}{\left(\frac{\gamma_L}{\gamma_D}\right)^2 ln2+\left[\frac{\nu-\nu_0}{\gamma_D}(ln2)^{1/2}-t\right]^2}dt \tag{4}$$

where ν is the wavenumber at which the cross section is being calculated. The pressure broadened linewidth at temperature T and pressure P is $\gamma_L = \gamma_0\left(\frac{P}{P_0}\right)\left(\frac{T_0}{T}\right)^{\alpha}$ where γ_o is the Lorentz linewidth at temperature T_0 and pressure P_0, and α the linewidth temperature dependence parameter. The Doppler broadened linewidth (HWHM) is $\gamma_D = \left(\frac{\nu_0}{c}\right)\left(\frac{2kTln2}{m'}\right)^{1/2}$ where $m'$is the mass of the molecule. The integral represents the convolution of the Gaussian and Lorentzian lineshapes. For this DIAL system, the Lorentz linewidth was retrieved from the HITRAN 2008 Database. Since the DIAL system makes all of its measurements horizontally, there is no variation in absorption cross section due to changes in pressure along the lidar's line of propagation. The linestrength S(T) is calculated with

$$S(T) = S_0\left(\frac{T_o}{T}\right)\left[\frac{1-\exp(-hc\nu_0/kT)}{1-\exp(-hc\nu_0/kT_0)}\right]exp\left[\frac{hc}{k}\left(\frac{1}{T_0}-\frac{1}{T}\right)E''\right] \tag{5}$$

where S_0 is the linestrength at temperature T_0, T is the temperature at which the line strength is being calculated, h is Planck's constant, ν_0 is the wavenumber associated with the absorption line center, k is Boltzmann's constant, and E'' is the energy above the ground state of the lower energy level associated with the absorption.

Care was taken in selection of the specific online and offline wavelengths to be used to minimize the sensitivity of the number density measurement to the atmospheric temperature that results from temperature dependence of the absorption cross section. Minimization of temperature sensitivity is advantageous for monitoring instruments such as the DIAL that in principle will make measurements in a variety of climates and seasons and thus a large range in ambient temperatures. To minimize sensitivity, temperature sensitivity of the absorption cross section was calculated as

$$\frac{1}{\sigma}\frac{d\sigma}{dT} \approx \frac{1}{T-T'}\frac{\sigma(T)-\sigma(T')}{\left(\frac{\sigma(T)+\sigma(T')}{2}\right)} \tag{6}$$

A plot of the sensitivity as a function of temperature is shown in Figure 2 based on the parameters listed in Table 1.

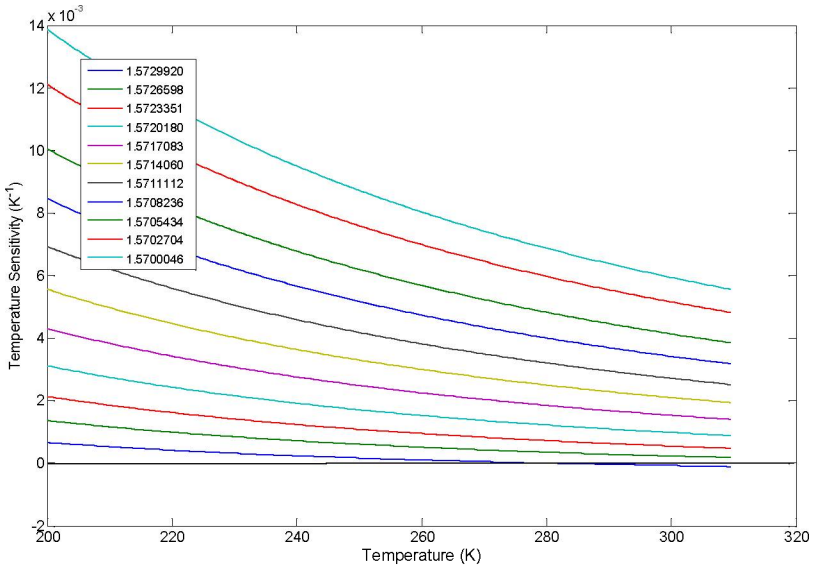

Figure 2 Plot of the temperature sensitivity of absorption lines in the absorption band of interest.

As can be seen on Figure 2, the absorption feature centered at 1.5708236 microns (lowest blue curve) is the least temperature sensitive around room temperature The 11 absorption line parameters for the lines plotted in Figure 1 as well as the water vapor lines within this range are tabulated in Table 1. The line chosen was 1.5714060 μm as shown in blue in Table 1. This line was chosen because it is one of the strongest absorption lines in the band and it does not have any overlapping water vapor absorption features. The cross section as a function of wavelength is shown in figure 3 with the online and offline wavelengths shown.

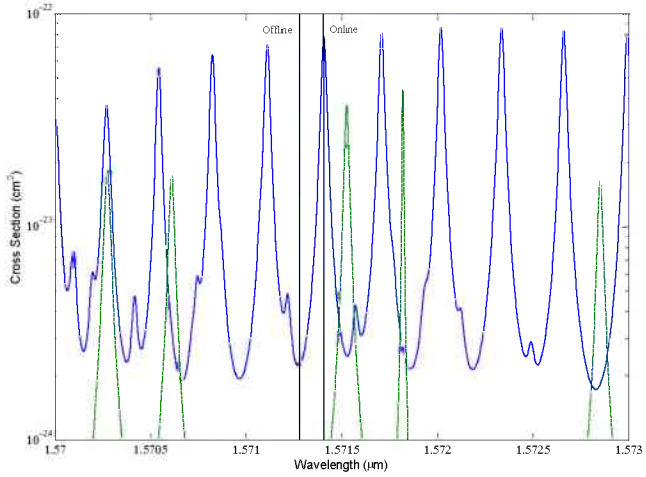

Figure 3 Plot of the cross section of CO_2 (blue) and water vapor (green) as a function of wavelength at 296 K and 0.85 atm.

Molecule	Line Center μm	Line Center cm^{-1}	Line strength x 10^{-23} cm^{-1} mol^{-1}	Lorentzian Linewidth (HWHM) cm^{-1}	Ground State Energy cm^{-1}	A
CO_2	1.5729920	6357.312	1.6600	0.0780	60.870	0.70
H_2O	1.5728510	6357.881	0.0034	0.0750	610.340	0.58
CO_2	1.5726598	6358.654	1.7300	0.0760	81.940	0.69
CO_2	1.5723351	6359.967	1.7400	0.0749	106.120	0.67
CO_2	1.5720180	6361.250	1.7100	0.0730	133.439	0.67
H_2O	1.5718192	6362.055	0.0026	0.0177	1327.110	0.06
CO_2	1.5717083	6362.504	1.6200	0.0729	163.868	0.69
H_2O	1.5715257	6363.243	0.0065	0.0625	1813.223	0.41
CO_2	1.5714060	6363.728	1.5100	0.0720	197.416	0.70
CO_2	1.5711112	6364.922	1.3700	0.0710	234.083	0.71
CO_2	1.5708236	6366.087	1.2200	0.0701	273.868	0.73
H_2O	1.5706108	6366.950	0.0037	0.0770	1122.709	0.53
CO_2	1.5705434	6367.223	1.0600	0.0700	316.770	0.74
H_2O	1.5702740	6368.315	0.0042	0.0840	982.900	0.56
CO_2	1.5702704	6368.330	0.9030	0.0900	362.788	0.82
CO_2	1.5700046	6369.408	0.7550	0.0880	411.923	0.82

Table 1: Parameters for selected CO_2 and H_2O absorption features near 1.57 μm from the HITRAN 2008 database[49]. These parameters were tabulated for a temperature of 296 K and an atmospheric pressure of 1 atm. The chosen absorption feature used for the CO_2 DIAL is highlighted in blue.

Dry Air Mixing Ratio Calculation

For a given DIAL measurement, the number density calculated from equation (3) is not as commonly used when discussing atmospheric carbon dioxide concentrations. Instead, typically concentrations are quoted in parts per million by volume. In order to convert the number density to parts per million, a calculation is made to estimate the total number of molecules present at the ambient pressure and temperature in a cubic centimeter of air using

$$PPM = 10^6 \left(\frac{N_d}{N_l}\right)\left(\frac{T}{273}\right)\left(\frac{101.33}{P}\right) \quad (7)$$

where N_d is the measured number density of CO_2, $N_L = 2.687 \times 10^{19}$ mol/cm^3 is Loschmidt's number which represents the number of air molecules in a cm^3 at T=296K and P=101.33 kPa, T is the ambient temperature in K, and P is the ambient pressure in kPa. It should be noted that this is for air, not dry air, which is a quantity typically of greater interest to those involved in atmospheric science. In order to calculate the parts per million of CO_2 by volume of all molecules in that volume excluding water vapor to yield the dry air mixing ratio, equation (7) must be modified to subtract out the number of water vapor molecules present in the volume giving

$$PPM = 10^6 \left(\frac{N_d}{N_L}\right)\left(\frac{T}{273}\right)\left(\frac{101.33}{P}\right)\left(\frac{1}{1-RHP(T)/P}\right) \quad (8)$$

where RH is the relative humidity, P(T) is the saturation pressure as a function of temperature for water vapor, and P is the ambient pressure.

Error Analysis

The error in the retrieved number density, $N_d(r)$, can be calculated using a differential error analysis. Starting with the DIAL equation

$$N_d(r) = \frac{1}{2\Delta r(\sigma(\lambda_{on},r)-\sigma(\lambda_{off},r))} ln\left(\frac{N(\lambda_{on},r)N(\lambda_{off},r+\Delta r)}{N(\lambda_{on},r+\Delta r)N(\lambda_{off},r)}\right) \quad (9)$$

assuming a constant online and offline cross section as a function of range, and defining $C = \frac{1}{2\Delta r(\sigma_{on}-\sigma_{off})}$, the error in the number density, $dN_d(r)$, as a function of the online and offline return signal is

$$dN_d(r)^2 = \left(\frac{\partial N_d(r)}{\partial N(\lambda_{on},r)} dN(\lambda_{on},r)\right)^2 + \left(\frac{\partial N_d(r)}{\partial N(\lambda_{off},r+\Delta r)} dN(\lambda_{off},r+\Delta r)\right)^2 + \left(\frac{\partial N_d(r)}{\partial N(\lambda_{on},r+\Delta r)} dN(\lambda_{on},r+\Delta r)\right)^2 + \left(\frac{\partial N_d(r)}{\partial N(\lambda_{off},r)} dN(\lambda_{off},r)\right)^2 \quad (10)$$

Evaluation of the partial derivatives in equation (10) based on equation (9) yields

$$dN_d(r)^2 = C^2\left[\left(\frac{dN(\lambda_{on},r)}{N(\lambda_{on},r)}\right)^2 + \left(\frac{dN(\lambda_{off},r)+\Delta r}{N(\lambda_{off},r+\Delta r)}\right)^2 + \left(\frac{dN(\lambda_{on},r)+\Delta r}{N(\lambda_{on},r+\Delta r)}\right)^2 + \left(\frac{dN(\lambda_{off},r)}{N(\lambda_{off},r)}\right)^2\right] \quad (11)$$

Assuming that the error in each signal measurement results from photon counting statistics allows one to write $dN(\lambda_{on},r) = \sqrt{N(\lambda_{on},r) + B(\lambda_{on})}$ where $B(\lambda_{on})$ is the sum of the dark count and background noise for $N(\lambda_{on},r)$ and is assumed constant as a function of range. A similar result can be written for the offline wavelength. Using these results, eq.(11) can be written

$$dN_d(r)^2 = C^2\left[\frac{N(\lambda_{on},r)+B(\lambda_{on},r)}{N(\lambda_{on},r)^2} + \frac{N(\lambda_{off},r+\Delta r)+B(\lambda_{off},r+\Delta r)}{N(\lambda_{off},r+\Delta r)^2} + \frac{N(\lambda_{on},r+\Delta r)+B(\lambda_{on},r+\Delta r)}{N(\lambda_{on},r+\Delta r)^2} + \frac{N(\lambda_{off},r)+B(\lambda_{off},r)}{N(\lambda_{off},r)^2}\right] \quad (12)$$

The dark count and background noise is measured for each wavelength by collecting photon counts for 3.75 μs before the laser pulse leaves the DIAL transmitter. This error analysis is used with the data presented later in this report.

III. The DIAL Instrument

The Laser Transmitter

The DIAL system, shown schematically in figure 4, consists of a laser transmitter and a DIAL receiver. The laser transmitter is based on an injection seeding erbium doped fiber amplifier (EDFA) with an optical pulse train and is described in this section.

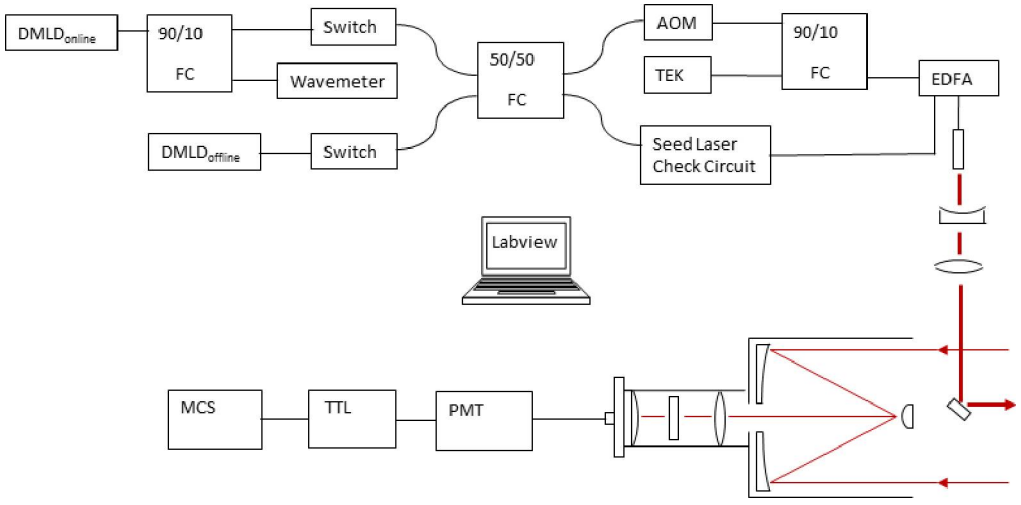

ACRONYM KEY

DMLD = Discrete Mode Laser Diode	TEK = Tektronics Source
FC = Fiber Coupler	PMT = PhotoMultiplier Tube
AOM = Acousto-Optic Modulator	MCS = MultiChannel Scaler
EDFA = Erbium Doped Fiber Amplifier	

Figure 4 Schematic of the DIAL system components.

The seeding begins with two tunable fiber pigtailed diode laser modules (Figure 5). The modules contain the laser diodes as well as a thermoelectric cooler (TEC) for temperature control of the laser diode and a built in optical isolator for protection against optical feedback. The laser modules are fiber pigtailed with polarization maintaining fiber and each laser module is mounted into a laser diode mount from ILX lightwave (ILX LDM-4980). The laser mounts themselves have a built in TEC for setting the baseplate temperature that the lasers are mounted on to. The laser diode mount TEC's are useful for setting the baseplate temperature near the laser diode temperature so that the smaller internal laser diode module TEC's do not require

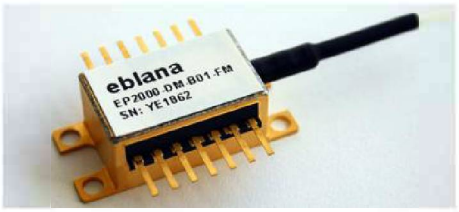

Figure 5 Seed laser diode module from Eblana Photonics (Part NO: EP1571-DM-BAA)

as much drive current to maintain the lasers at a given temperature. Each baseplate TEC in controlled with a Wavelength Electronics temperature controller (WTC3253). During normal operation, the online laser is set to an operating temperature of 48.14 degrees Celsius, and the offline laser is set to 54.57 degrees Celsius. The laser diode TEC's for both lasers are controlled by an ILX Lightwave 3742B laser diode driver. These laser diode drivers set and hold the laser diode temperature with a proportional, integral, derivative (PID) loop control. For normal laser operation, the diode mount temperature was set to minimize the drive current through the laser diode TECs. This was done to improve the temperature stability of the laser diodes, and was set by adjusting the laser diode mount temperature set point while monitoring the laser diode TEC drive current until the drive current reached a minimum value. Once the operating temperatures were set for stable single mode laser operation, the temperatures were not adjusted.

Of the two seed lasers, one laser diode is set at the offline wavelength and one laser is set at the online wavelength. The lasers have a factory specified linewidth of approximately 2 MHz. For validation, measurements were made of the seed laser effective linewidth using a self-heterodyne linewidth measurement. The results of these measurements for the online and offline seed lasers are shown in figures 6 and 7 respectively.

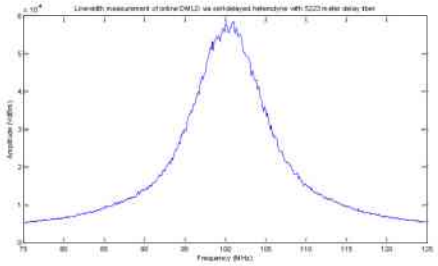

Figure 6 RF spectrum of the delayed self-heterodyne measurement of the online laser using a 5223 meter long delay fiber.

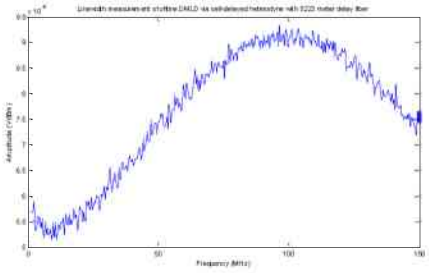

Figure 7 RF spectrum of the delayed self-heterodyne measurement of the offline laser using a 5223 meter long delay fiber.

With this measurement the online laser had a measured linewidth (full width half maximum) of 10 MHz, and the offline laser had a measured linewidth of 150 MHz. The discrepancy between the measured linewidth and the factory specified linewidth was attributed to the fast frequency jitter in the carrier frequency.

Switching between the offline and online wavelengths was accomplished with a combination of two computer controllable fiber optic signal switches (Agiltron LB 1x1, LBSW-115171323) and a 50/50 fiber coupler. Switching was done with two 1x1 signal switches as opposed to using a 2x1 switch because 2x1 switches have a dead time at their output as they switch from one input to the other (Figures 8 and 9). This is not desirable for the fiber amplifier, as the dead time for low loss mechanical switches, on the order of several milliseconds, is too long for the amplifier to operate without a seeding signal. With two independent switches acting as simple on off switches, the second laser switch can be enabled and given enough time to produce an output before the first switch is disabled (Figures 8 and 9).

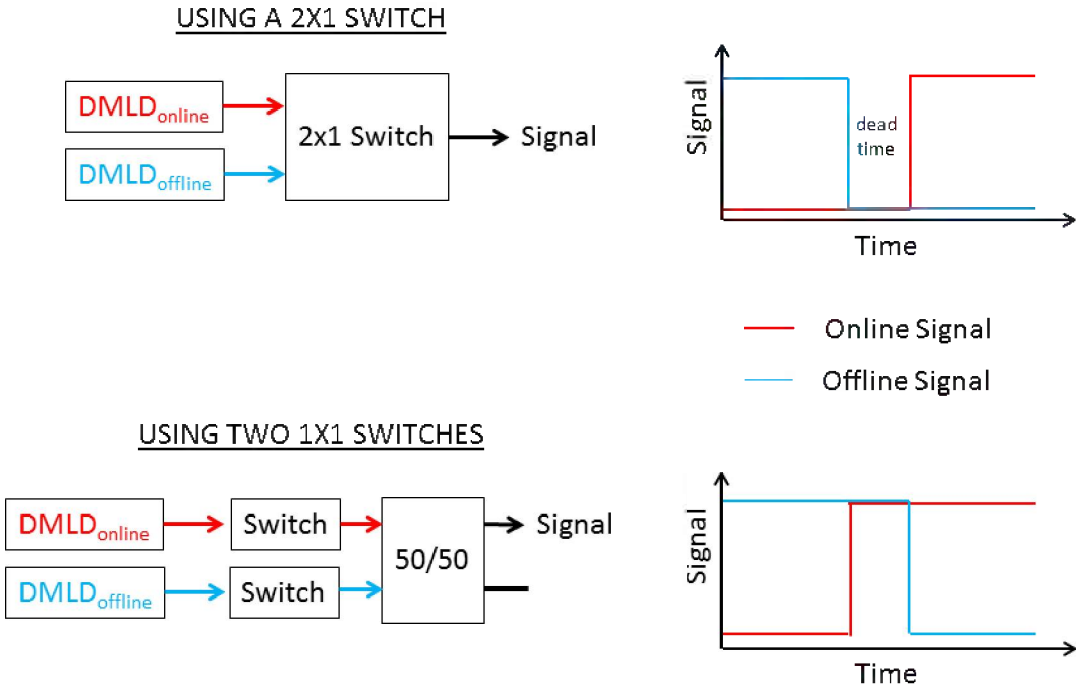

Figure 8 Comparison of using two 1x1 switches vs. a 2x1 switch. A 2x1 switch has an unacceptable dead time when switching between one input and the other that would be detrimental to the EDFA performance.

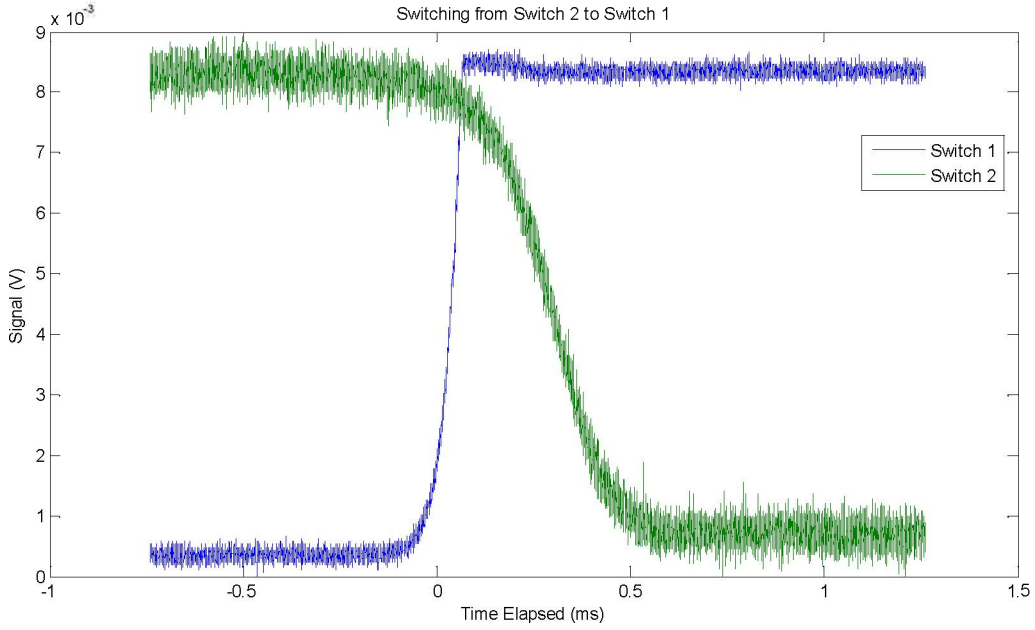

Figure 9 Screen shot of the switching scheme used by the DIAL with two 1x1 switches. By turning the second switch on before turning the first switch off the EDFA is continuously seeded.

In this way, the amplifier always has a seed signal to maintain stable operation of the amplifier. As is depicted in Figure 9, for 0.5 ms the amplifier is being seeded with two wavelengths. The

lidar data produced during this brief window of time is useless for DIAL measurements since both wavelengths are present in the backscattered signal. A signal switch is employed to discard any data collected during this time period of dual wavelength operation. After the fiber optic switches, a 50/50 fiber coupler (Thorlabs 10202A-50-APC) is employed to provide an optical path for either diode laser to seed the amplifier. The other end of the 50/50 coupler that is not directed towards the AOM and EDFA is connected to a seed laser check circuit. A schematic of this check circuit is shown in figure 10. One output of the 50/50 fiber coupler is connected to a Thorlabs D400FC optical detector. The analog output of this detector is monitored by a custom made seed laser check circuit. This circuit is connected to the interlock of the EDFA, and if no optical signal is present which represents the seed signal not going into the EDFA, the seed laser check circuit disables emission of the EDFA by opening the interlock with a relay. This protects the EDFA from operating without a seed laser, which can potentially damage the EDFA. This circuit is shown in figure 11.

Figure 10 Block diagram of the seed laser check circuit.

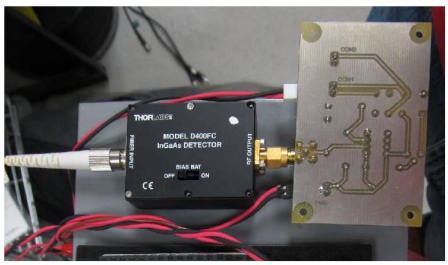

Figure 11 Photo of the seed laser check circuit attached to the optical detector.

The seed lasers are run CW for frequency stability, but, the lidar itself requires a pulsed light source. To generate a train of optical pulses, a fiber pigtailed acousto-optic modulator (AOM) made by Brimrose (AMM-100-20-25-1573-2FP) is used to convert the CW signal in to a pulse train. When power is not applied to the AOM, no optical signal leaves the output fiber. To transmit the input optical signal to the output fiber, an RF electrical driving signal is applied to the electrical connection of the AOM module. This signal modulates an acoustic transducer on the side of a section of glass that the light is propagating through. The acoustic wave forms a grating that the incident light beam scatters from, and the first order scattered beam is coupled in to the fiber optic output.

The AOM operates effectively as a fast on/off switch, which chops the CW input signal from the seed lasers in to an optical pulse train. For the DIAL the AOM is modulated on and off with an AOM driver made by Isomet connected to a pulse train generator (Stanford Research Systems DG645). The pulse train generator is easily configured through its user interface for arbitrary pulse durations and repetition rates, allowing the user a high level of control over the lidar pulse characteristics. The trigger output from the pulse train generator also synchronizes the AMCS USB data acquisition unit to the lidar pulses. For normal operation, the pulse duration is set to 200 ns which is the minimum pulse duration the AOM can generate, and the pulse repetition rate is set to 15 kHz.

During normal operation, the seed lasers will slowly drift in operating wavelength 10's of pm over the course of several hours. To correct for small drifts, as well as to repeatedly set the online laser's operating wavelength at the center of the absorption line being used for the DIAL,

a 90/10 fiber coupler is used just after the online laser's output to sample a small fraction of the online laser light with a wavemeter (Burleigh WA-1500, later replaced by a Bristol 621).

During data collection periods, the wavelength measured with the wavemeter is read by the controlling PC via a GPIB connection. If the wavelength is measured to be outside a user specified tolerance, typically 0.5 pm, the diode current for the online laser is adjusted until the laser is back within the tolerance window. The WA-1500 wavemeter can measure an absolute laser wavelength with a precision of 36.4 MHz. During typical data collection periods, the offline laser wavelength is set with the wavemeter before the data collection period, and then is not monitored again during data collection since its exact wavelength is not as critical to the DIAL measurement as the online laser's wavelength is.

The laser pulse train at the output of the AOM first passes through a 90/10 fiber coupler, which has its other input connected to a Tektronics tunable diode laser source (LPB 1100). The Tektronics source is set to emit 1 mW of fiber coupled laser light at 1560 nm. The reason for having this source in the fiber optic train is that the EDFA has a built in input power monitoring circuit designed to disable amplifier emission in the absence of a seed laser signal of sufficient intensity. The EDFA used is a CW amplifier, and it expects to see a CW seed laser signal. For the DIAL however, the pulses injected in to the amplifier are not long enough in duration to register a signal on the EDFA's built in power monitor. To seed with our signal and bypass the built in power monitoring, the Tektronics source is used to put a signal that the EDFA's built in power monitor will see, but, since the 1560 nm light is well outside the amplifier's optical gain bandwidth, the 1560 nm light does not get amplified to contaminate the EDFA output spectrum. As stated previously, the EDFA is a commercial CW fiber amplifier designed for telecommunications applications (IPG Photonics EAR-K-L, Figure 12). The amplifier is

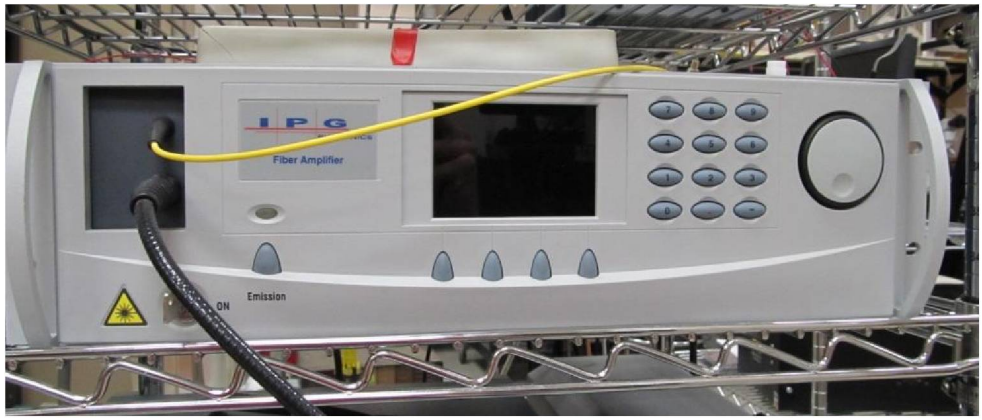

Figure 12 IPG Photonics EAR-5K-L Erbium doped fiber amplifier used for the DIAL.

capable of operating in either a constant power or constant gain mode. In constant power mode, the gain of the amplifier is adjusted automatically to maintain a fixed power output. In constant gain mode, the pump diode current in the amplifier remains fixed, and the output power is neither monitored nor adjusted. For the DIAL, the amplifier is being operated in constant gain mode. When the input is a pulse train instead of a CW input, the amplifier was found to operate erratically in constant power mode, as the output power monitor within the amplifier does not accurately measure the pulsed output power and as a result tended to dramatically overshoot the

desired output power risking damage to the amplifier. In constant gain mode, the pump diode current was adjusted to typically 1.50 Amps to reach the desired average output power.

A parameter of concern with all EDFA's is the Stimulated Brillouin Scattering threshold. Stimulated Brillouin Scattering (SBS) is a non-linear optical effect where a forward propagating light wave can generate an acoustic Bragg grating in the fiber core that can completely backscatter all of the originally forward propagating optical energy. The backscattered energy is often in the form of high peak power pulses which are capable of destroying optical components. SBS requires a minimum light intensity before the process can generate sufficiently large acoustic gratings to be a problem. This minimum light intensity is the SBS threshold, and for fiber optic cables that confine optical beams to very small areas, this threshold can be less than 1 mW. To measure the threshold of the EDFA, the setup depicted in Figure 13 was employed. The measurement uses a fiber coupler to measure the spectral content of any backreflected light coming out of the input of the EDFA. When SBS occurs, the backscattered light is redshifted from the incident light by roughly 10 GHz, which is typical for silica glass fibers. This allows discrimination between input light that has been backreflected by Fresnel reflections at fiber junctions and light that has been scattered through SBS processes. The optical spectrum of the backscattered light was measured while either the gain of the amplifier or the magnitude of the seed laser power was gradually increased. Well below the SBS threshold, the spectrum consists only of the seed wavelength shown in figure 14. Approaching the SBS threshold, a small shoulder occurs offset from the peak on the red side by 10 GHz seen in figure 15. Normal DIAL operation is safely below this SBS threshold to protect the optical components from potential damage.

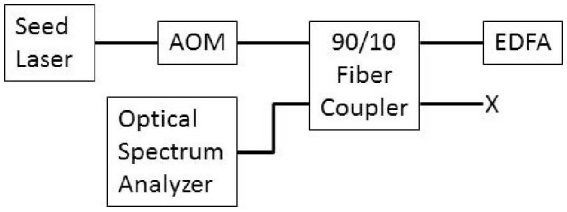

Figure 13 Block diagram for the measurement of the SBS threshold

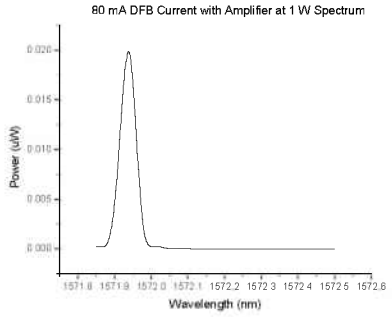

Figure 14 Measured signal with setup shown in Figure 13. Below the SBS threshold only the seed laser wavelength is present.

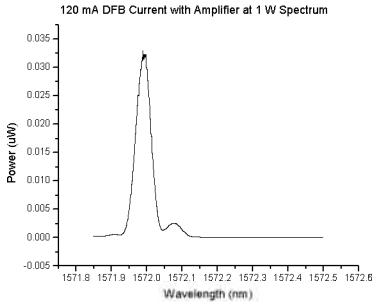

Figure 15 When the SBS threshold is crossed, red-shifted backscattered light is observed as a shoulder on the long wavelength side of the seed laser signal.

Another problem identified with the EDFA was the temporal and spectral content of the output. Ideally, the amplifier would simply produce an amplified version of the input signal. In practice, this was not found to be the case. The output pulse train was found to have a non-zero temporally varying amplified spontaneous emission (ASE) output between pulses. The severity of the problem depended heavily on the gain of the amplifier as seen in figure 16. To low of a gain and the majority of the optical power at the output was ASE based. At higher gains the problem was lessened.

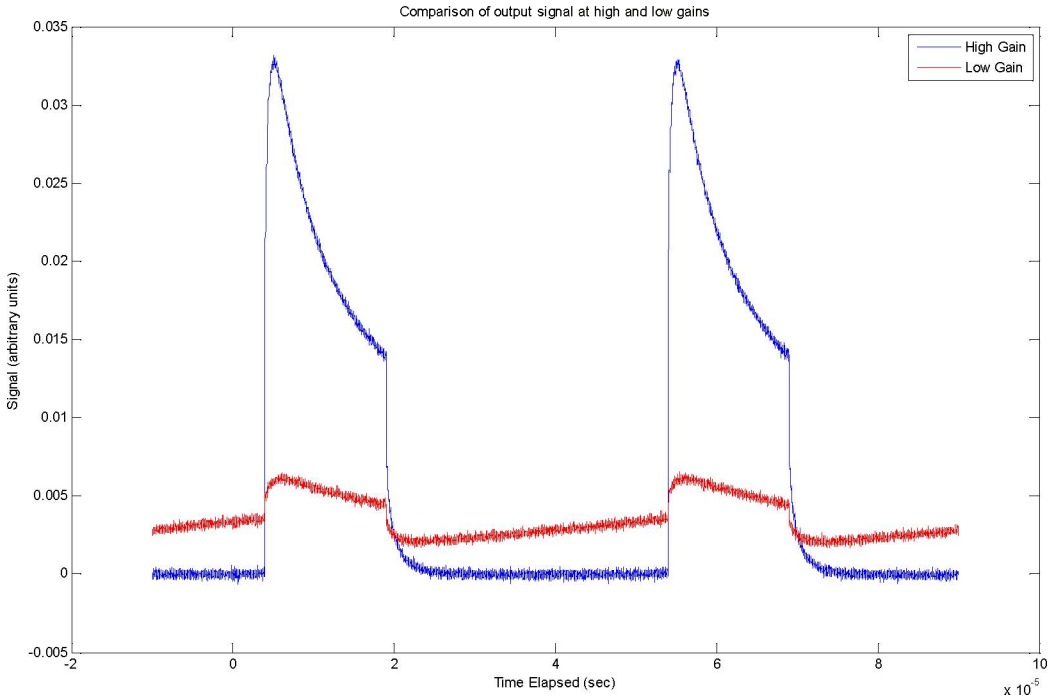

Figure 16 Optical signal emitted from the EDFA at high and low gain settings. At lower gains, ASE emission dominates (red curve). At higher gains this problem is reduced (blue curve)

This type of output was found to be highly disruptive to accurate DIAL measurements, as it introduced a time varying background noise on top of the backscattered signal which was impossible to completely remove in the data processing. To minimize this output in between pulses, the gain was adjusted until the output between pulses was found to be as small as possible. This occurred at a pump diode current setting of 1.50 A. The remaining ASE in between pulses was measured to be nearly completely filtered by the narrow band filter in the DIAL receiver. This pulse train is shown in figure 17. This was attributed to the fact that the EDFA ASE spans the EDFA's gain spectrum which ranges from 1571-1575 nm, while the filter has a full width half maximum transmission of only 0.9 nm and is centered at 1571.52 nm at room temperature which is at the lower end of the EDFA's gain spectrum.

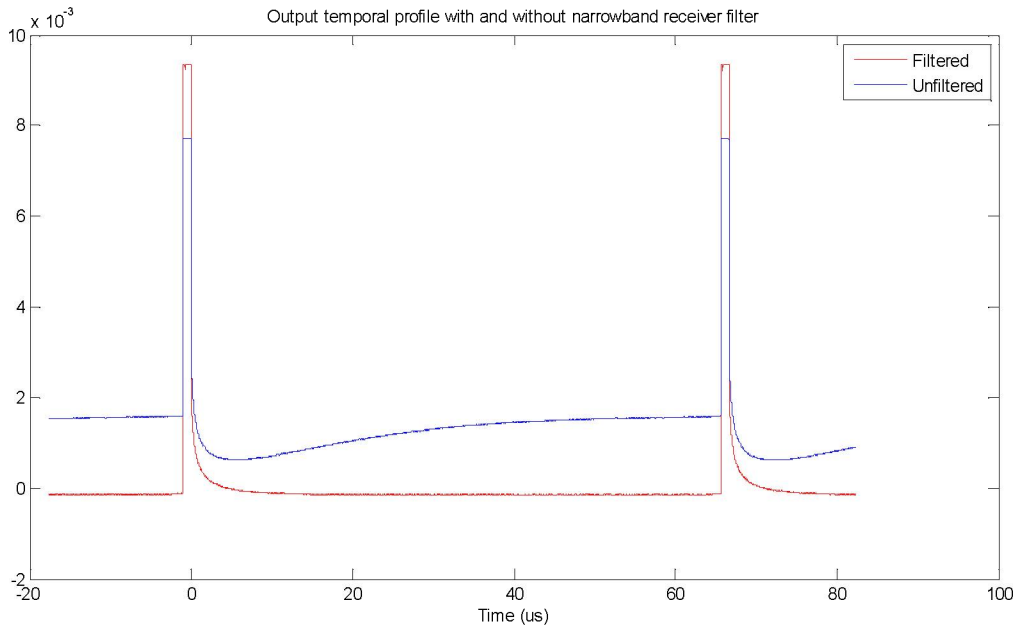

Figure 17 Filtered (red curve) and unfiltered (blue curve) output of the EDFA.

Under normal operation, the laser transmitter output pulse parameters are listed in Table 2.

Pulse Duration	200	ns
Pulse Energy	65	μJ
Repetition Rate	15	kHz
Wavelength (online/offline)	1.5714069/ 1.5712585	μm

Table 2: Transmitter pulse parameters used during normal operation.

A major design goal for the DIAL was to build an instrument that was eye safe under normal operation. Since the DIAL will be scanning horizontally over large areas that will often contain sequestration site personnel, reducing the DIAL's irradiance to eye safe levels to maintain the health and safety of personnel is critical. At 1.5 microns, the eye safe requirements from the American National Standards for Safe Use of Lasers (ANSI-Z136.1-1993) laser safety guidelines require a maximum permissible exposure (MPE) of 6.67 μJ/cm^2. A maximum exposure time of 10 seconds was assumed in making the eye safety calculations, as this is the expected maximum exposure time per the ANSI guidelines for non-visible beams where an individual would be visually unaware they are under the exposure of potentially hazardous radiation.

The fiber output of the EDFA is attached to a fiber collimator optical assembly which nominally collimates the output beam to a diameter of 5 mm. The radiation emitted from the EDFA is too high in irradiance to be considered eye safe. To correct this, a 10x beam expander was employed to increase the beam diameter from 5 mm to 50 mm. The EDFA fiber collimator

assembly was connected to the beam expander with a custom machined mount shown in figure 18.

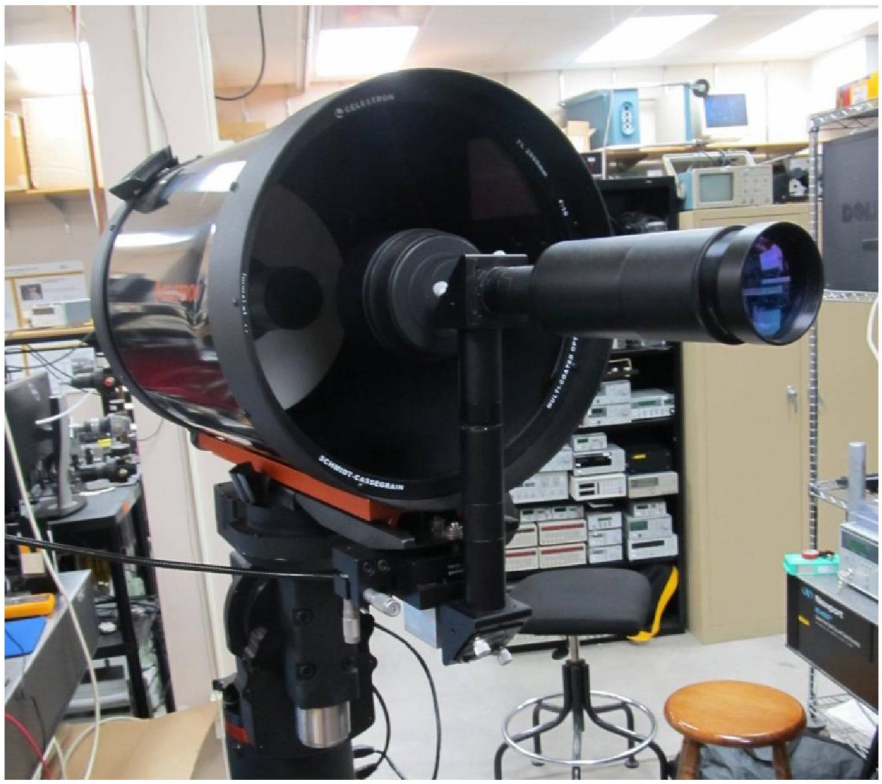

Figure 18 Another photo of the beam expander mounted to the telescope. The beam is entirely contained within SM1 optical tubing until it has been expanded to an eye-safe diameter of 5 cm.

At this new diameter, the DIAL pulses are reduced to 3.36 μJ/cm^2, which is within the eye safe guidelines. The beam expander consists of a -50 mm focal length plano-convex lens and a -25 mm plano convex lens paired together for achieving fast beam divergence. Another 200 mm focal length plano convex lens is employed to collimate the DIAL output at an eye-safe diameter.

The form of the beam expander was chosen for several reasons. First, it was desirable for transmitted pulses to be fired coaxially with the optical axis of the receiver. When the pulse first exits the DIAL, it is possible depending on the optical configuration to have a large initial burst of stray light be captured by the receiver. This is undesirable for the low light level detectors employed for photon counting, as the magnitude of this initial burst of light can be large enough to cause damage in PMT's. When the light is launched coaxially, the obscuration of the secondary mirror on the Schmidt-Cassegrain telescope used reduces this initial flash to manageable levels.

The beam expander is mounted on a tip tilt stage to align the outgoing beam with the optical axis of the receiver. The tip/tilt stage was mounted to the side of the telescope because it was found that using the alignment screws on the final turning mirror of the expander altered the received lidar signal used for alignment since the user's arm partially obscures the receiver aperture while they are making the screw adjustments. To correct this, the beam steering adjustments were placed outside of the receiver's field of view so that during transmitter

alignment, the user could make alignment adjustments without obscuring any of the receiver's field of view. The turning mirrors used were silver coated instead of dielectrically coated mirrors to reduce polarization sensitivity of the transmitted pulse energy. The EDFA uses non-polarization maintaining fiber, which causes the output polarization of the amplifier to drift during operation, especially during the first several minutes of operation when the amplifier is settling in to a thermal steady state.

DIAL Receiver

The receiver portion of the DIAL begins with an 11 inch Schmidt-Cassegrain telescope made by Celestron (CGE-XLT-11). This telescope can be seen in figure 18. The Schmidt-Cassegrain style was selected primarily for its compact form which was better suited to field deployment than larger forms such as the Newtonian telescope. A plano-convex lens acts to collimate the light collected by the telescope for optical filtration. After the collimating lens, a narrow band optical filter (Barr Associates) with an optical transmission full width half maximum of 0.9 nm is used. The filter transmission as a function of wavelength is shown in figure 19. This filter serves to improve the optical signal to noise ratio by suppressing the out of band light that would otherwise be incident on the detector from both the atmosphere and the ASE from the EDFA. After the received light is filtered, it is fiber coupled with an aspheric lens module (Thorlabs PAF-11-X-APC) in to a 1000 mm fiber for the PMT detector or a 105 micron diameter fiber for the APD

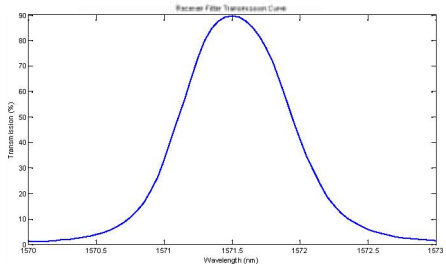

Figure 19 Transmission curve of the narrowband filter used to filter EDFA amplified spontaneous emission and ambient light.

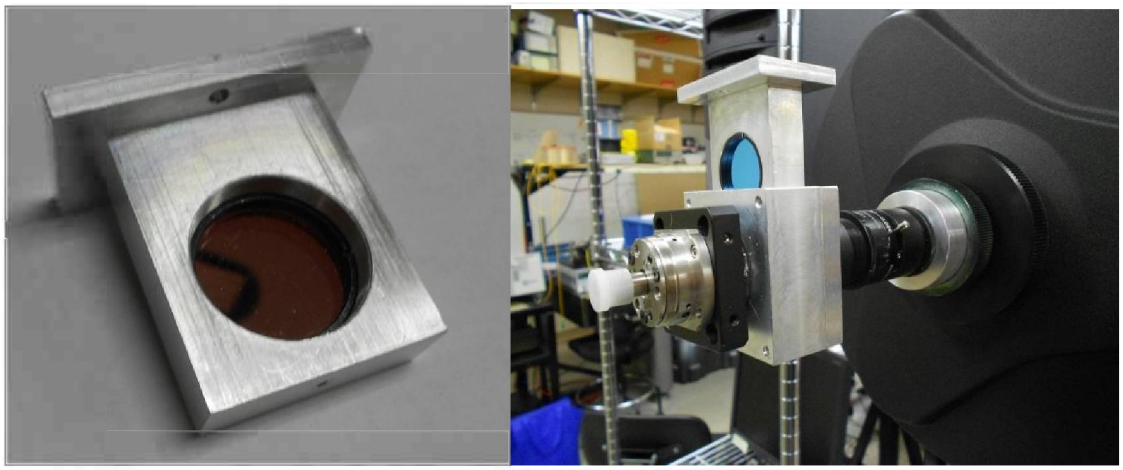

Figure 20 The narrowband optical filter in its housing (left) that can be removed for alignment of the DIAL from the receiver optical train (right)

module. A picture of the optical receiver train is shown in figure 20 and includes the custom filter mount. The 1000 mm multimode fiber used for the PMT module is made by Ocean Optics and this large core diameter was selected to ease initial alignment and data collection with the DIAL. The drawback of using such a large core fiber is that it opens the field of view of the

telescope allowing more background light to be collected by the receiver, but, for nighttime data collection this difference in background light was found to be negligibly small.

The detector used with the 1000 micron core fiber is a near infrared photomultiplier tube (PMT) module made by Hamamatsu Corporation (H10330-075A). For DIAL data collection, the PMT is operated in the Geiger mode where it measures individual photons captured by the DIAL receiver. To reduce the dark count rate to 200 kHz on average the module cools the photocathode to -50 degrees Celsius. For normal operation, the PMT was adjusted to operate at 800 volts for photon counting. When a photon triggers a photoelectron avalanche within the PMT, the signal output of the PMT contains a small voltage spike generated by the photoelectron avalanche. This spike is captured by a Hamamatsu C9744 photon counting module that generates a 50 ns duration square 5 volt pulse at its output to signal the detection of a photon if the voltage spike is above a user controlled discrimination voltage level, normally 200 mV. This unit operates as an interface between the PMT whose output is analog, and the data acquisition device used for DIAL data collection which measures digital signals.

For DIAL data collection, the output of the C9744 is monitored and recorded by a multi-channel scaler card (Sigma Space Corporation AMCS-USB). The lidar signals vary rapidly on time scales of 10's of ns, and the DIAL often monitors the atmosphere for temporal periods of several hours. If this was recorded directly, this would generate tremendous amounts of data to process and store. To reduce the amount of data to more manageable levels, the scaler card performs inboard range binned averaging over many thousands of laser shots and transfers the averaged single data set to the PC, reducing the amount of data to manage considerably. On a given laser shot, the scaler card is triggered 3 microseconds before the AOM is enabled by the same pulse train generator used to generate the control modulation signal for the AOM. After identifying the trigger pulse, the scaler card counts rising edges of digital pulses and bins the counts in time bins of 50 ns. The number of range bins worth of data to collect is set by the user. When the next trigger pulse is registered by the scaler card, the scaler again counts and range bins the measured pulses adding them to the recorded range binned data from the previous laser shot. This process of adding the next laser shot's photon counts to the previous laser shots' continues for a user specified number of accumulation cycles. When the number of laser shots is equal to the number of user specified number of accumulates, the scaler card writes the data to a buffer to be read over a USB connection by a PC.

There is a limitation for using a single data acquisition channel on the scaler card in that if the DIAL operating wavelength is switched in the middle of an accumulation cycle, the integrated data set that is transferred to the PC will be a mix of online and offline returns, making this data useless for computing CO_2 concentrations. If the online and offline wavelengths are switched frequently, which is usually the case, these wasted accumulation cycles can significantly tax the percentage of accumulated data that is not contaminated, requiring longer real time acquisition periods to get good signal to noise from temporal averaging. To bypass this limitation, an RF signal switch (Mini-Circuits ZX80-DR230-S+) is employed to route the output of the C9744 to either channels one or two of the scaler card with channel one dedicated to accumulating online data and channel two dedicated to accumulating the offline data (Figures 21 and 22). The output from the C9744 discriminator is routed to either channel 1 if online signals are being collected or channel 2 if offline signals are being collected.

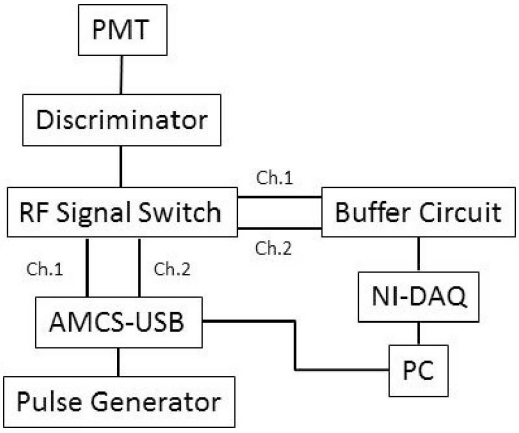

Figure 21 Block diagram for the RF signal routing switch.

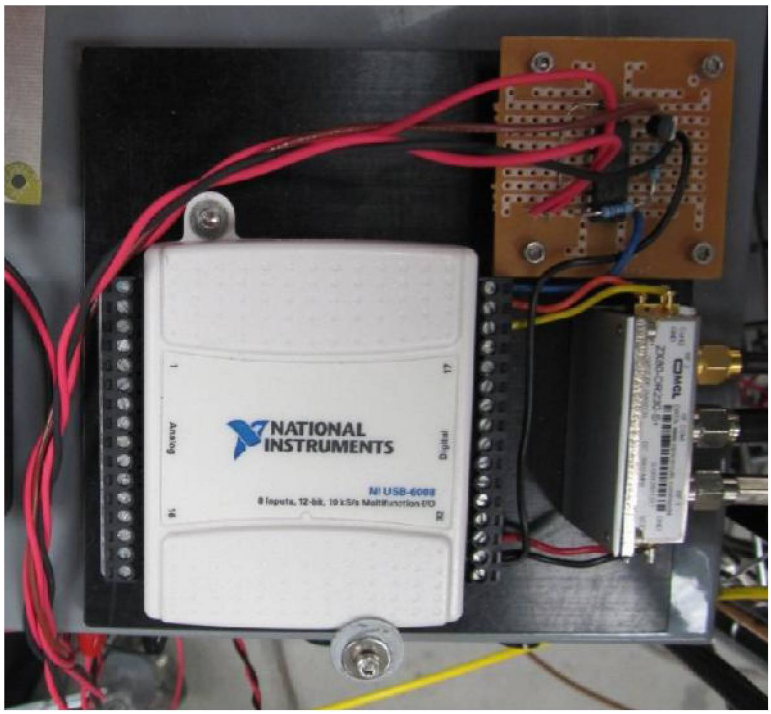

Figure 22 Photo of the RF signal switch, buffer circuit, and NI-DAQ control card.

The routing of the data is controlled by Labview with a National Instruments IO card (National Instruments, NI USB-6008). The IO card was found to not be capable of sourcing enough current to fully engage the RF signal switch channels on and off, so a buffer circuit was introduced between the IO card and the RF signal switch to supply the additional control current.

When switching between the online and offline wavelengths, there is a brief period where both wavelengths are seeding the DIAL system as described in the previous sections. When this is occurring, both RF signal switch outputs are set to the off position, so no data is accumulated

during this brief period. Use of this switch allows the user to switch wavelengths at arbitrary rates, regardless of the settings and accumulation periods of the scaler card.

Data Acquisition and Processing

The DIAL instrument collects data using a Labview based program that operates in the following manner. The on-line injection seeding laser is locked to the on-line wavelength as described below. The 20 MHz MCS integrates the return signal using range bins of 7.5 m (50 ns time bins) for a user defined time, typically 1 – 10 seconds. The 200 ns pulse generated by the EDFA amplifier corresponds to a 30 m range resolution implying that the MCS is oversampling. The summing of the 7.5 m bins is performed during the post processing where bins are added together to achieve the range resolution for the DIAL instrument. To maintain good signal to noise, an increasing range bin size as a function of range is used. Data is collected for 3.75 μs before the laser pulse leaves the DIAL instrument allowing the background level to be measured. The computer then reads the integrated MCS signal and stores this data as a row in a matrix. This data is also displayed on the front panel of the Labview program in a waterfall plot allowing the operator to monitor the return signal. The switch to the off-line wavelength is then opened followed by the closing of the switch to the on-line wavelength. This is done sequentially so that the EDFA is always seeded, which avoids potential damage from stimulated Brillioun scattering and amplified spontaneous emission . The off-line data is then integrated using the MCS for the user defined time, and this data is read and stored as the next row in the data matrix. This process is repeated until the data collection program is stopped.

Locking of the on-line wavelength for DIAL measurements is achieved using the cw output from the DMLD laser monitored by the wavemeter. The operating wavelength of the injection seeding DMLD laser is monitored using a Labview based program that reads the wavemeter. The operating wavelength of the DMLD laser is compared to a set-point wavelength creating an error signal. The operating wavelength of the DMLD laser is corrected using the error signal to adjust the current to the DMLD laser via a GPIB interfaced current controller. A plot of the on-line wavelength as a function of time using this locking scheme is shown in figure 23. This locking scheme is capable of maintaining the operating wavelength of the DMLD laser to within ±70 MHz for extended periods of time.

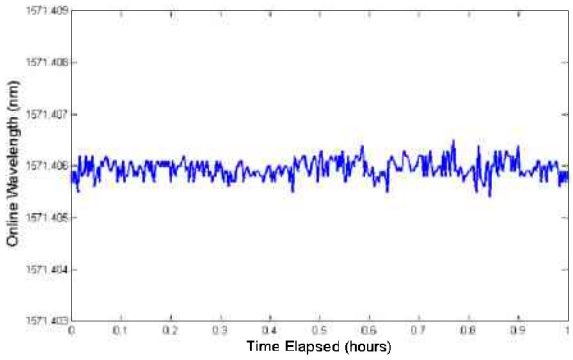

Figure 23 A plot of the operating wavelength as a function of time for the DMLD laser with the locking engaged. The control loop for locking can maintain the operating frequency of the DMLD laser to within ±70 MHz over a 60 minute time period.

IV. DIAL Data

DIAL Instrument Cargo Trailer

The DIAL instrument was deployed near the Zero Emission Research Technology (ZERT) field site for the summer 2011 release experiment. The DIAL instrument was housed in a cargo trailer shown in figure 24. The cargo trail was partitioned into two haves using a removable wall with a form insulation. Housed in the front of the trailer, which was enclosed by the insulating partition was the electronic rack containing the laser transmitter, the wavelength locking components, the photomultiplier tube (PMT), the miscellaneous electronic components, and the computer used to control and log data. Contained within the back of the trailer, which contains the ramp access was the scanning mount that contained the fiber coupled output and turning mirror for the co-linear outgoing optical beam, the collecting telescope, and the receiver optical train. The light collected by this receiver optical train was fiber coupled and brought back to the PMT in the front part of the trailer. This arrangement allowed the electronic components to be insulated from the large daily temperature swings that occur in Bozeman, Montana due to the high altitude and relatively dry climate. These temperature swings can range between 0 C at night to 35 C. Pictures of the DIAL instrument deployed in the two sections of the cargo trailer are shown in figure 25 and 26. The CO_2 DIAL instrument was deployed at a

Figure 24 The cargo trailer housing the CO_2 DIAL instrument shown at its field

Figure 25 The electronics rack housed in the front of the trailer. A desk was also contained in this section for the instrument operator.

Figure 26 The scanning mount housing the output beam optics, telescope, and optical receiver train in the back of the trailer. The generator (seen in the lower right hand part of the trailer) was used to provide power to operate the instrument.

remote site located well away from the ZERT controlled release facility with no available facilities. A portable generator, seen in the low left hand portion of the trailer in figure 26,was used to supply the power needed to operate the DIAL instrument.

Field Experiment

A subsurface controlled release experiment was performed between July 18 and August 15, 2011 at the ZERT controlled release facility on the western edge of the Montana State University campus. The sub-surface control rate for the summer 2011 release experiment was 0.15 tons CO_2/dat release equally in the six sections of the buried release pipe. A Google Earth map of the location of the cargo trailer housing the DIAL instrument relative to the controlled release facility is shown in figure 27. The CO_2 DIAL instrument was located approximately 1.25 km from the ZERT site. Data with the DIAL instrument was collected primarily during the evening hours to minimize operating the DIAL instrument when personnel were located on the field. This mode of operation was followed even though the DIAL instrument meets the eye-safety standards presented in American National Standard for Safe Use of Lasers (American National Standards Institute ANSI Z136.1-1993 (section 8)) Minimum Permissible Exposure (MPE).

Figure 27 The CO_2 DIAL instrument relative to the ZERT site for the summer 2011 controlled

Experimental Results

Validation of the DIAL instrument was conducted by placing the Licor LI-820 sensor at the ZERT field site. The DIAL instrument was the operated over the ZERT field site. Time series of data was then collected with the both the Licor LI-820 sensor and the DIAL. These time series where than compared to validate the DIAL data. To first get an idea of the signal-to –

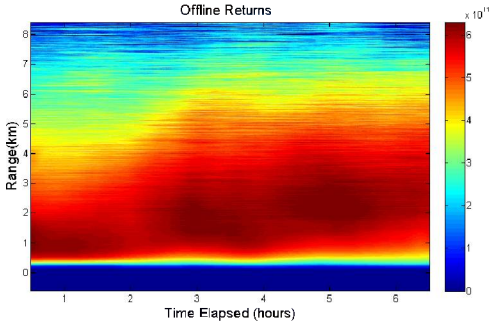

Figure 28 The range corrected return signal as a function of time for the off-line wavelength over a seven hour period

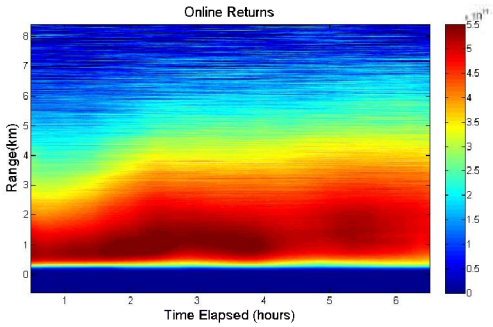

Figure 29 The range corrected return signal as a function of time for the off-line wavelength over a seven hour period

noise performance of the DIAL instrument, the return signal was collected as a function of range and time for the off-line wavelengths as shown in figure 28 while the range corrected returns as a function of range and time are shown in figure 29. A range corrected profile for the on-line and off-line wavelengths are shown in figure 30.

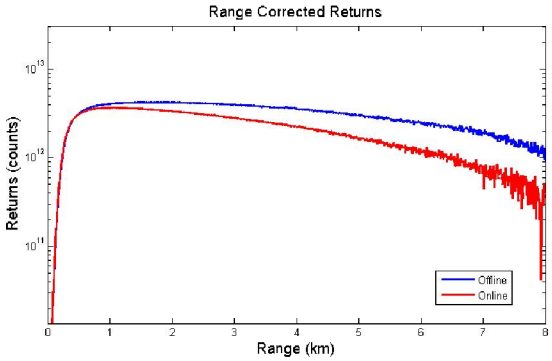

Figure 30 Range corrected returns as a function of the range for the on-line (red) and off-line (blue) wavelengths.

The error bars for the CO_2 profile can be estimated by using the return signal and the photomultiplier tube characteristics on the following manner. The DIAL instrument uses photon counting to monitor the return signal at both the on-line and off-line wavelengths. Using counting statistics, the average photon number and deviation can be calculated at each range bin. Using these average photon numbers, their deviations, and the DIAL equation the CO_2 concentration and its corresponding error can be calculated. A plot of the measured CO_2 concentration as a function of range is shown in figure 31. A plot of the expected signal to noise performance from the original proposal is shown in figure 32.

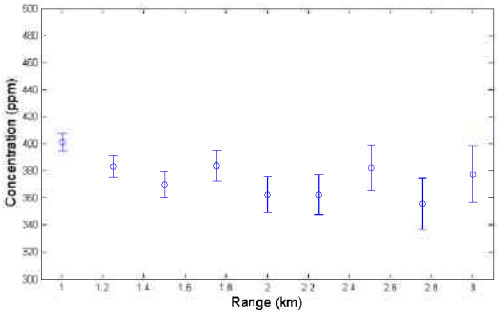

Figure 31 Measured CO_2 concentration as a function of range with the associated error bars.

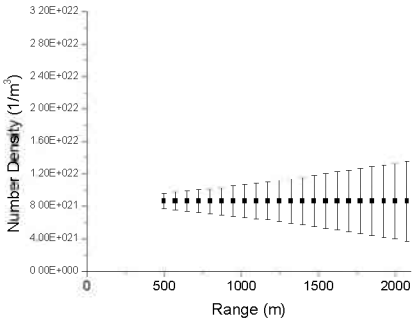

Figure 32 Expected signal to noise performance from the original proposal. (Note 8.22×10^{21} $1/cm^3$ corresponds to a 400 ppm CO_2

Validation of the DIAL instrument data was achieved by comparing the Licor LI-820 sensor with the DIAL data as a function of time at the range bin associated with the ZERT release site where the Licor was located. Three time series plots of CO_2 concentration as a function of time measured with the Licor LI-820 shown as the red lines and the DIAL measurements shown as the blue lines are shown in figure 33-35. Reasonable agreement the DIAL and Licor measurements indicate the DIAL is able to monitor CO_2 concentrations at the ZERT controlled release experiment.

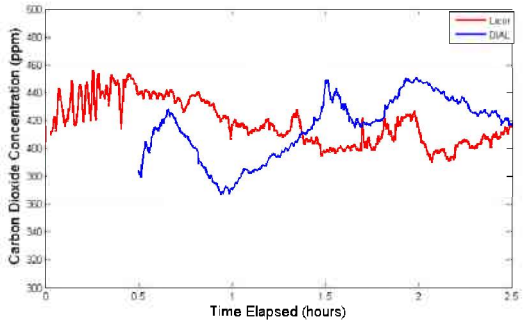

Figure 33 A comparison of the CO_2 concentration as a function of time measured using the Li-Cor LI-820 sensor (red Line) and the DIAL instrument (blue line) over a 2 hour period. The Licor LI-820 was located at the ZERT field site.

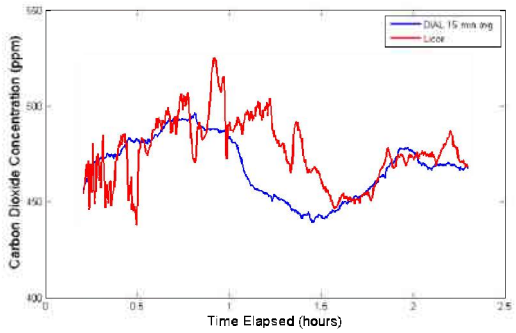

Figure 34 A comparison of the CO_2 concentration as a function of time measured using the Licor LI-820 sensor (red Line) and the DIAL instrument (blue line) over a 2.5 hour period. The Licor LI-820 was located at the ZERT field site.

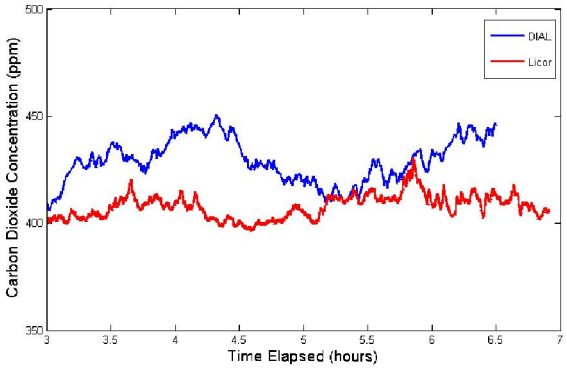

Figure 35 A comparison of the CO_2 concentration as a function of time measured using the Licor LI-820 sensor (red Line) and the DIAL instrument (blue line) over a 4 hour period. The Licor LI-820 was located at the ZERT field site.

The DIAL instrument was deployed at the ZERT site during the controlled release experiment in the summer of 2012.. A 1.8 kW generator was used to operate the instrument and the instrument was located over 1 km away from the release facility. A plot of the CO_2 concentration as a function of range is shown in figure 36. The error bars shown in figure 46 are calculated as described above. A plot of the CO_2 number density as a function of time is shown in figure 4 for data collected at 1 km away from the DIAL instrument. The DIAL instrument measurement is represented by the blue line with accompanying error bars while the co-located Licor 820 point sensor, shown at the ZERT site in figure 37, measurement located 1 km away from the DIAL instrument is represented by the red line. Good agreement between these two measurements indicates the DIAL instrument is operating correctly.

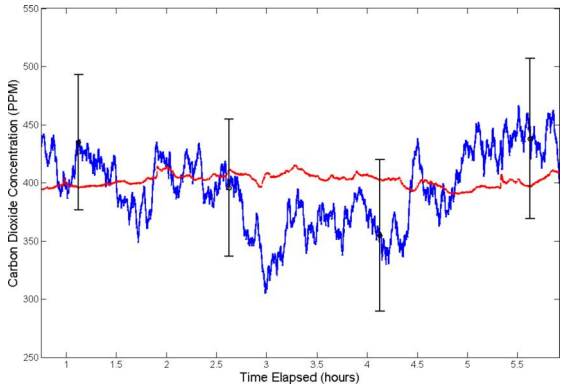

Figure 36 CO_2 number density as a function of time for the DIAL instrument (blue line) for the 1 km range bin and the Licor 820 point sensor (red line).

A plot of the CO_2 concentration as a function of time is shown in figure 38 with the DIAL instrument data represented by the blue line while the Licor data is represented by the red line. Again, good between the two measurements indicates that the DIAL is operating correctly and can see changes in the CO_2 concentration.

Figure 37 The Licor 820 sensor placed at the ZERT site. The inlet tube is at the top of the post to the left of the

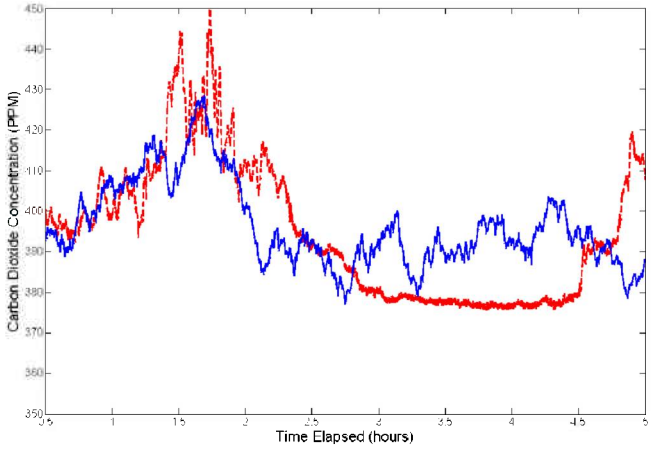

Figure 38 CO_2 number density as a function of time for the DIAL instrument (blue line) and the Licor 820 point sensor (red line). The DIAL is able to detect temporal changes in the CO_2 concentration.

The DIAL instrument was transported and set up at the Big Sky Carbon Sequestration Partnership site in North Central Montana, near the towns of Kevin and Oilmont. The students operating the instrument stayed at the nearest hotel in the town of Shelby, approximately 30 miles to the south. A Google map image of the location of the instrument deployment is shown in figure 39. The DIAL instrument was located approximately 1 km from the approximate site of the future production well. The DIAL was housed in a cargo trailer. A picture of the instrument deployed in the cargo trailer and an image looking out from the cargo trailer over which the DIAL operated is shown in figure 40. Because of the lack of facilities such as electricity, the DIAL instrument was operated using a 2 kW generator. The generator was able to operate several hours at a time on a tank of gas and, because of this operational duration of the generator and the distance to the accommodations, the DIAL was operated over several hours each day.

Figure 39 Map of the deployment site at the BSCSP site near Kevin, MT.

Figure 40 The left hand picture shows the DIAL instrument deployed in the cargo trailer at the BSCSP site while the right hand picture shows the view from the cargo trailer over which the DIAL was operated. The approximate site of the future production well will be approximately 1 km away from the where the trailer was located and would be in view of the left hand picture.

Data collected on July 22, 2013 is shown in figures 41-43. A plot of the on-line and off-line return signals are shown in figure 41. The blue line and red line represents the off-line and on-line return signal as a function of range respectively. The corresponding number density profile

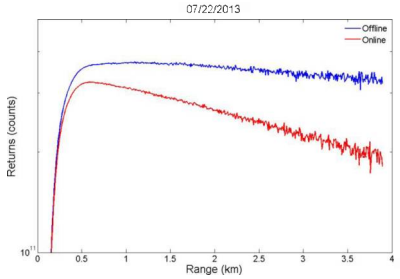

Figure 41 The return signal as a function of time for data collected July 22nd. The blue (red) line indicates the off-line (on-line) return signal.

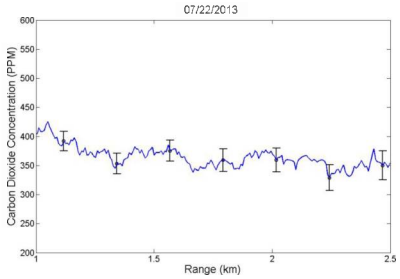

Figure 42 The CO_2 concentration as a function of range retrieved using the on-line and off-line return signals shown in figure 51.

retrieved from the data shown in figure 41 is shown in figure 42. The error bars on the CO_2 profile shown in figure 4 result from a differential error analysis. A plot of the CO_2 concentration as a function of time and range is shown in figure 43 for data collected on July 22. The collection time for this data was limited by the operational time of the generator which was limited by the gas tank capacity.

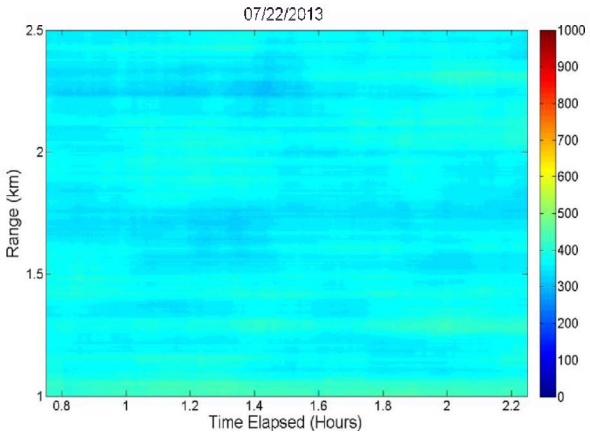

Figure 43 The CO_2 concentration as a function of

Data collected July 26 is shown in figures 44-47. A plot of the on-line and off-line data for data collected July 26th is shown in figure 44 with the blue line and red line representing the off-line and on-line returns respectively.

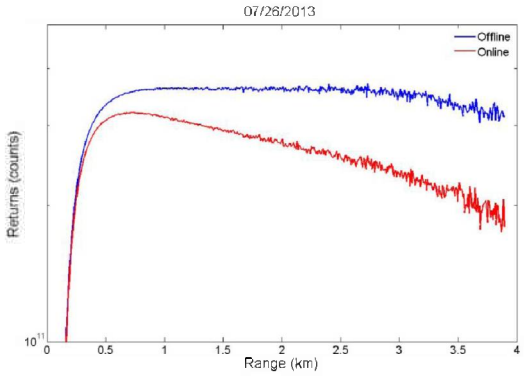

Figure 44 The return signal as a function of time for data collected July 26th. The blue (red) line indicates the off-line (on-line) return signal.

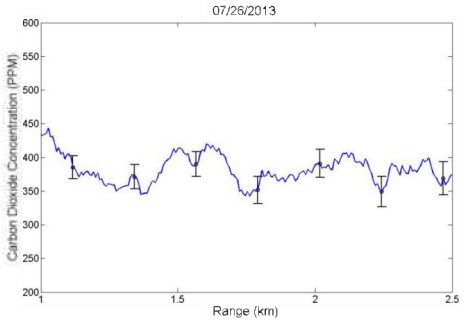

Figure 45 The CO_2 concentration as a function of range retrieved using the on-line and off-line return signals shown in figure 54.

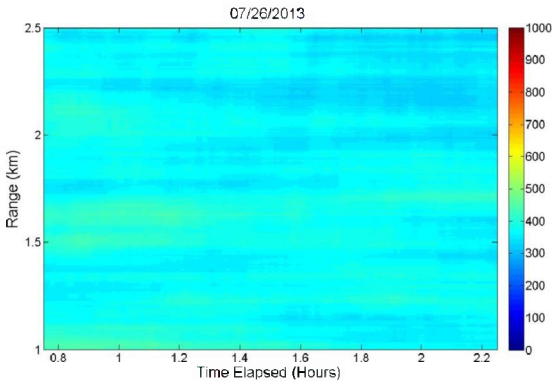

Figure 46 The CO_2 concentration as a function of range and time for July 26th.

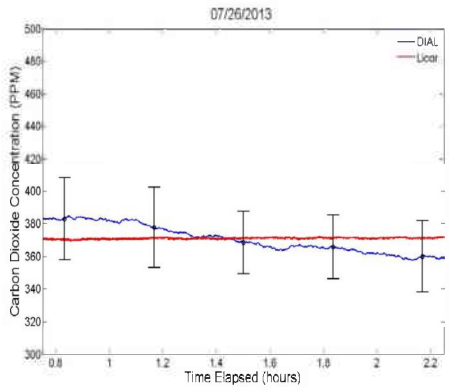

Figure 47 The CO_2 concentration measured with the DIAL is shown as the blue line while the CO_2 concentration measured by the Licor is shown as the red line.

Using this data, the CO_2 concentration as a function of range is shown in figure 45. Again, the error bars shown in figure 45 are based on a differential error analysis. The CO_2 concentration as a function of time and range is shown as the false color plot shown in figure 46. As seen in both figure 45 and figure 46, the CO_2 concentration remains relatively constant over the data collection period as there is no local sources or sinks of CO_2. As a validation of the DIAL data, the Licor CO_2 point sensor was deployed as part of the data collection. A comparison of the CO_2 concentration as a function of time is shown in figure 47 as the blue line with the error bars calculated based on a differential error analysis. The red line indicates the CO_2 concentration measured using the Licor point source detector. Agreement between these two instruments to within the error bars associate with the DIAL retrieval indicate the DIAL instrument is working properly.

The DIAL instrument can be scanned using the computer controlled scanning motors in the tripod mount. Initial scan data was collected at the BSCSP site. The CO_2 concentration as a function of range for the scan data is overlaid on a Google map of the field site and is shown in figure 48.

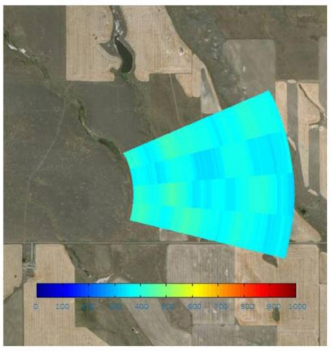

Figure 48 The CO_2 concentration as a function of spatial location overlaid on a google map of the field site. This data was collected using the scanning capability of the DIAL.

V. Conclusion

A DIAL instrument for spatially monitoring carbon dioxide number densities has been developed. This DIAL instrument uses diode lasers to injection seed an EDFA to produce the pulsed online and offline signals. The DIAL receiver collects the light scattered in the atmosphere and monitors as a function of time the return signal at both the online and offline wavelengths allowing the DIAL equation to be employed to produce a range resolved number density profile for CO_2.

The DIAL instrument has been deployed at both the ZERT and Big Sky Carbon Sequestration Partnership sites. Data from the DIAL has been validated using a co-located Licor Li-820 point sensor indicating the DIAL instrument is operating appropriately. Work on improving the signal to noise capability of the DIAL instrument continues as a new detector is being incorporated into the DIAL receiver to replace the current PMT which, currently limits the DIAL performance.

Appendix A: Papers/Thesis

"Differential Absoprtion Lidar (DIAL) for Carbon Dioxide Monitoring", William Johnson, Kevin S. Repasky, and John L. Carlsten, Applied Optics, Vol. 52 Issue 13, pp.2994-3003 (2013).

Development of a Differential Absorption Lidar for Identification of Carbon, William Eric Johnson, Ph.D. Thesis, Montana State University, November 2013.

Appendix B: Talks

"Development of a Differential Absorption Lidar (DIAL) for Carbon Sequestration Site Monitoring", William Johnson, Amanda Bares, Amin R. Nehrir, Kevin S. Repasky, and John L. Carlsten, American Geophysical Union, San Francisco, California, 2011.

"Development of a scanning differential absorption lidar for monitoring carbon sequestration site integrity", Will Johnson, Kevin S. Repasky, and John L. Carlsten, Annual Conference on Carbon Capture Utilization and Sequestration, Pittsburg, PA, April 2012.

"Development and deployment of a compact eye-safe scanning differential absorption lidar (DIAL) for spatial mapping of carbon dioxide for monitoring/verification/accounting at geologic sequestration sites", Kevin S. Repasky, John L. Carlsten, William Johnson, and Amanda Bares, Carbon Storage R&D Project Review Meeting, Pittsburgh, PA, August, 2012.

"Development and deployment of a compact eye-safe scanning differential absorption lidar (DIAL) for spatial mapping of carbon dioxide for monitoring/verification/accounting at geologic sequestration sites", Kevin S. Repasky, John L. Carlsten, William Johnson, and Amanda Bares, Carbon Storage R&D Project Review Meeting, Pittsburgh, PA, August, 2013.

"Development and Testing of a Scanning Differential Absorption Lidar For Carbon Sequestration Site Monitoring", Benjamin Soukup, William Johnson, Kevin S. Repasky, and John L. Carlsten, American Geophysical Union, San Francisco, CA, 2013.

"Optical Tools and Techniques for Large Area Surface Monitoring of Carbon Sequestration Sites", Kevin S. Repasky, William Johnson, Benjamin Soukup, John L. Carlsten, Rick Lawrence, and Scott Powell, Optical Society of America, Energy and the Environment, Tucson, AR, 2013.